Aperture configuration optimization for extended scene observation by an interferometric telescope

Hiyam Debary, Laurent Mugnier, Vincent Michau

Optics Letters

Aperture configuration optimization for extended scene observation by an interferometric telescope

Hiyam Debary,* Laurent M. Mugnier, and Vincent Michau

Office National d'Études et de Recherches Aérospatiales, B.P. 72, 92322 Châtillon, France
**Corresponding author: hiyam.debary@onera.fr*

Received 6 May 2022; revised 23 June 2022; accepted 12 July 2022; posted 13 July 2022; published 5 August 2022

In this Letter, we aim at optimizing the aperture configuration of an optical interferometric imager for observing extended objects. We exploit combinatorial theory results from different authors to prove the existence of solutions to some problems of aperture configuration optimization in dimension 1. We determine in which cases these solutions exist for a compact frequency coverage and provide an explicit solution whatever the number of apertures. We apply these results and provide an illustration in two cases: the first is an interferometer composed of radially disposed arms; and the second consists of an innovative hybrid architecture involving a small monolithic telescope, which covers short spatial frequencies added at the center of the first case design. Last, we carry out an analysis to determine under which condition a monolithic telescope placed at the center of this hybrid instrument can complete its frequency coverage without gaps.

https://doi.org/10.1364/OL.462561

The acquisition of the first successful interferences from two separate apertures dates back to the Albert Michelson and Francis Pease experiment in 1921 [1]. The elementary measurement, called an interferogram [2], is generated through the combination of the light from two different apertures separated by a given distance, called a baseline. The characteristics of the interferogram, which are the contrast and the position of the fringes, can be grouped into a physical quantity called the complex visibility. Using the van Cittert–Zernike theorem [3], and in the absence of atmospheric turbulence, one can directly link the complex visibility to the Fourier transform of the "source", at a spatial frequency given by the baseline and the wavelength.

The principle of an interferometric imager is to measure multiple complex visibilities from multiple baselines, and thus sample the Fourier transform of the observed source. In astronomy, optical long baseline interferometry uses this principle with baselines between a few large telescopes. Famous examples of such instruments include ESO's Very Large Interferometer Telescope (VLTI) [4], the Navy Precision Optical Interferometer (NPOI) [5], and Georgia State University's Center for High Angular Resolution Astronomy (CHARA) [6]. Astronomers rely on the super synthesis principle [7] where the rotation of the Earth during an observation night is used in order to increase the number of measured spatial frequencies.

Recently, another application of interferometry has emerged, where a traditional telescope making snapshot images is substituted by a pupil plane interferometer in which all spatial frequencies are measured simultaneously. The signal is collected by joint apertures and combined through photonic integrated circuits (PICs), allowing a significant increase in the number of spatial frequency measurements, in contrast to astronomical interferometers. In the so-called SPIDER (segmented planar imaging detector for electro-optical reconnaissance) demonstrator by Lockheed Martin [8–11], the apertures are evenly disposed in one-dimensional arrays, called arms in the following. Each arm is associated with a PIC which combines apertures, used at most once, by pairs. The arms are radially disposed, as represented in Fig. 1. In the following, we shall call such an interferometer SPIDER-like.

The set of measured spatial frequencies, called frequency coverage, is a key aspect in the design of the interferometer, and should be tailored to the type of source observed. In such an interferometer, the spatial frequencies are sampled with a step of b/λ, with b the distance between two consecutive apertures. For simplicity purposes, we will henceforth consider normalized spatial frequencies in units of b/λ. In this Letter, we consider the interferometric observation of a very extended source such as the Earth, viewed from a satellite. In this framework, Harvey and Rockwell [13] introduced the "practical resolution limit" (PRL), defining it as the inverse of the maximum spatial frequency before which no zero occurs in the optical transfer function. Indeed, few priors are available for a very extended source, making it necessary to have no gaps in the frequency coverage. We qualify such a frequency coverage as compact [14,15].

The list of combined aperture pairs in the instrument is hereafter called an aperture configuration. Lockheed Martin's aperture configuration, as described in Ref. [12], is presented in Figs. 2(a) and its associated frequency coverage in 2(b), where some medium and high spatial frequencies are missing. A different aperture configuration was suggested in Refs. [16–18] for the same SPIDER-like design with a frequency coverage producing only every other spatial frequency, and is presented in Figs. 2(c) and 2(d). In the above-mentioned SPIDER-like designs, each arm has the same aperture configuration and thus the same frequency coverage. Furthermore, each spatial frequency is formed at most once. Finally, in the case of the aperture configuration

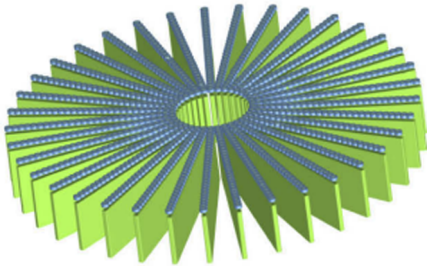

Fig. 1. Segmented planar integrated optical imaging system design with 37 one-dimensional arrays of 30 apertures (figure from Ref. [12]).

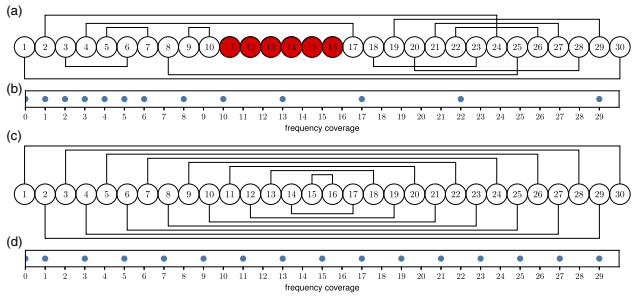

Fig. 2. (a) Aperture configuration of an interferometric arm of the SPIDER-like instrument as described in Ref. [12]. The black lines represent aperture pairings. The unused apertures are colored in red. The associated frequency coverage is represented in (b). (c) Aperture configuration as described in Refs. [16–18], with the associated frequency coverage in (d).

presented in Fig. 2(a), not all apertures are used and the frequency coverage presents many gaps even in the first half of the spectrum. A satisfactory reconstruction of these spatial frequencies would require strong priors on the object, such as the knowledge that it has a reduced support on a dark background. As a consequence, none of these two aperture configurations is suitable for very extended objects.

Two non-radial architectures have also been proposed. The first is a hexagonal array of apertures with a spiral pattern [19], providing a compact structure and a different frequency coverage. This architecture requires in-development two-dimensional PICs, which excludes it from our scope as we aim at using existing linear PICs. The second architecture is one with a T-shape array of apertures and produces non-simultaneous measurements [20]. In our study, we restrict ourselves to snapshot instruments and thus this design is not appropriate.

In this Letter, we aim at optimizing the frequency coverage of two types of flat instruments aiming at observing the Earth. The first is a SPIDER-like interferometer substituting a traditional telescope. The second is a hybrid instrument made of a traditional but smaller telescope which we complement with a SPIDER-like snapshot telescope. From the SPIDER-like description provided in Fig. 2, we keep the radially disposed arm architecture with the same aperture configuration shared between each arm, as well as the single use of each aperture for the simplicity of the device. We also keep the uniqueness of each spatial frequency measured, to avoid spatial frequency redundancy. In contrast, we wish to use all apertures available in order to broaden the spatial frequency coverage, i.e., to maximize the PRL. A major difference of our work with respect to that of previous authors, e.g., Refs. [16,18], lies in the fact that our optimization will be over all possible aperture configurations.

The number of aperture configurations scales exponentially with the number of apertures, thus it is impossible to carry out a systematic exploration. For instance, for 40 apertures, there are 12 521 965 697 different frequency coverages [21]. In the following, we present an original approach based on combinatorial theory results obtained by several authors [21–25], to solve the problem whatever the number of apertures and provide an associated example of aperture configuration. Then, we apply this approach to optimize the frequency coverages of both the above-mentioned instruments.

As we consider configurations where each aperture is used once and once only, the total number of apertures N_p must be even, given that they are connected by pairs. The number of measured spatial frequencies is thus $N_\mathrm{p}/2$ in the range $[1, N_\mathrm{p} - 1]$. A buildable frequency coverage is defined as one that has an aperture configuration leading to it. Note that each frequency coverage is not buildable.

For instance, a frequency coverage of the form $\{\ldots, N_\mathrm{p} - 2, N_\mathrm{p} - 1\}$ is trivially not buildable. Indeed, the two outer apertures have to be connected in order to measure the $N_\mathrm{p} - 1$ spatial frequency, leaving a next maximal measurable spatial frequency of $N_\mathrm{p} - 3$.

We first wish to find buildable frequency coverages that have a compact structure, i.e., that are composed of consecutive spatial frequencies $\{1, 2, \ldots, N_\mathrm{p}/2\}$. This problem has been formulated and solved in the framework of combinatorial theory by Skolem [22], and such a frequency coverage is called a Skolem set and its associated aperture configuration a Skolem sequence.

More generally, for the applications presented in this Letter, we wish to build frequency coverages in the form $\{n_\mathrm{min}, n_\mathrm{min} + 1, \ldots, n_\mathrm{min} + N_\mathrm{p}/2 - 1\}$, where n_min is the first measured spatial frequency. This problem has been introduced by Langford [26], and such a frequency coverage is called a Langford set and its associated aperture configuration a Langford sequence. The existence of buildable compact frequency coverages was solved for $n_\mathrm{min} = 1$ by Skolem in 1958, for $n_\mathrm{min} = 2$ by Davies [23] in 1959, then partially generalized by Bermond [24] in 1978, and finally completed by Simpson [25] in 1983.

To sum up the results derived by these authors, a frequency coverage of the form $\{n_\mathrm{min}, n_\mathrm{min} + 1, \ldots, n_\mathrm{min} + N_\mathrm{p}/2 - 1\}$ is buildable if and only if

$$4n_\mathrm{min} \leq N_\mathrm{p} + 2, \tag{1}$$

yielding a condition on the highest minimum spatial frequency for n_min,

$$n_\mathrm{min} \leq \left\lfloor \frac{N_\mathrm{p} + 2}{4} \right\rfloor \triangleq n_\mathrm{min}^\mathrm{max} \tag{2}$$

and any of

- $N_\mathrm{p} \equiv 0\,(\mathrm{mod}8)$,
- $N_\mathrm{p} \equiv 2\,(\mathrm{mod}8)$ and n_min odd,
- $N_\mathrm{p} \equiv 6\,(\mathrm{mod}8)$ and n_min even.

The first condition translates into having a maximal first spatial frequency of $\frac{N_\mathrm{p}+2}{4}$ and thus the highest spatial frequency of $\frac{3N_\mathrm{p}-2}{4}$. One explicit aperture configuration is provided in Refs. [22–25] given the values of N_p and n_min defining the frequency coverage, as follows.

- $n_\mathrm{min} = 1$:

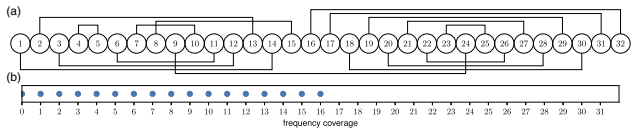

Fig. 3. (a) Example of a Skolem aperture configuration with 32 apertures. (b) Associated frequency coverage ranging from 1 up to 16.

- $N_p \equiv 0\,(\mathrm{mod}8)$: see first part of proof of theorem 2 [22]
- $N_p \equiv 2\,(\mathrm{mod}8)$: see second part of proof of theorem 2 [22]
- $N_p \equiv 4\,(\mathrm{mod}8)$: no solution [22]
- $N_p \equiv 6\,(\mathrm{mod}8)$: no solution [22]

• $n_{\mathrm{min}} = 2$:
- $N_p \equiv 0\,(\mathrm{mod}8)$: see first part of proof of theorem 2 [23]
- $N_p \equiv 2\,(\mathrm{mod}8)$: no solution [23]
- $N_p \equiv 4\,(\mathrm{mod}8)$: no solution [23]
- $N_p \equiv 6\,(\mathrm{mod}8)$: see second part of proof of theorem 2 [23]

• $n_{\mathrm{min}} > 2$:
- $N_p \equiv 0\,(\mathrm{mod}8)$:
  * $n_{\mathrm{min}} \equiv 0\,(\mathrm{mod}4)$: see first table of Ref. [25]
  * $n_{\mathrm{min}} \equiv 1\,(\mathrm{mod}4)$: see fourth table of Ref. [25]
  * $n_{\mathrm{min}} \equiv 2\,(\mathrm{mod}4)$: see second table of Ref. [25]
  * $n_{\mathrm{min}} \equiv 3\,(\mathrm{mod}4)$: see third table of Ref. [25]
- $N_p \equiv 2\,(\mathrm{mod}8)$:
  * $n_{\mathrm{min}} \equiv 0\,(\mathrm{mod}2)$: no solution (as mentioned before) [24]
  * $n_{\mathrm{min}} \equiv 1\,(\mathrm{mod}2)$: see second table under theorem 2 [24]
- $N_p \equiv 4\,(\mathrm{mod}8)$: no solution (as mentioned before) [24]
- $N_p \equiv 6\,(\mathrm{mod}8)$:
  * $n_{\mathrm{min}} \equiv 0\,(\mathrm{mod}2)$: see first table under theorem 2 [24]
  * $n_{\mathrm{min}} \equiv 1\,(\mathrm{mod}2)$: no solution (as mentioned before) [24]

In Code 1, Ref. [27], we provide the reader with a tool exhibiting aperture configurations given n_{min} and N_p.

In the Skolem case ($n_{\mathrm{min}} = 1$), the measured spatial frequencies are $\{1, 2, \ldots, N_p/2\}$ and thus the frequency coverage is buildable if and only if $N_p \equiv 0$ or $2\,(\mathrm{mod}8)$.

As a first step, we focus on a rewiring of the first SPIDER-like design considered in order to increase the PRL. We study the case of a compact frequency coverage starting at the spatial frequency 1, i.e., the above defined Skolem configuration. As $N_p = 30$ does not satisfy the congruity condition given above, we consider the closest working case $N_p = 32$. Using the constructive solution from the first half of the proof of theorem 2 in Ref. [22], we provide an illustrative aperture configuration in Fig. 3. In summary, this aperture configuration achieves a compact frequency coverage in contrast to SPIDER, and improves the PRL as it is no longer equal to 6, but 16.

As a second step, we aim at further optimizing the PRL obtained in the first SPIDER-like design studied. In that sense, we consider the hybrid instrument constituted of the interferometer complemented with a small monolithic telescope measuring short spatial frequencies.

More specifically, we no longer wish to consider frequency coverages starting at the spatial frequency 1 but rather as high as possible considering the low spatial frequencies are measured by the monolithic telescope, to improve the resolution of the device. In the general case, if buildable, the Skolem configuration reaches $N_p/2$ by definition and the Langford configuration reaches $(3N_p - 2)/4$ as a consequence of Eq. (1). Because the maximum spatial frequency measured increases

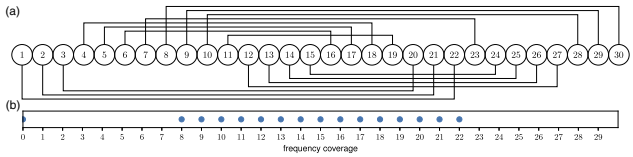

Fig. 4. (a) Example of a Langford configuration with 30 apertures. (b) Associated frequency coverage ranging from spatial frequencies 8 up to 22.

from $N_p/2$ to $(3N_p - 2)/4$, the resolution of this hybrid interferometer is improved by approximately 50% with respect to the interferometer with the Skolem configuration. Maintaining the SPIDER-like interferometer aperture complexity, i.e., $N_p = 30$ as presented in Fig. 2, we apply these results and we aim at finding a compact frequency coverage with the highest minimum spatial frequency, $n_{\mathrm{min}}^{\mathrm{max}}$, as defined in Eq. (2). A consequence of the latter is that $n_{\mathrm{min}}^{\mathrm{max}} = 8$ for $N_p = 30$. Using the first table under theorem 2 in Ref. [24], we provide an illustration of this Langford aperture configuration in Fig. 4. The represented aperture configuration produces a compact frequency coverage ranging from spatial frequencies 8 to 22, improving the frequency coverage provided by a Skolem configuration, i.e., by substantially extending the highest spatial frequency.

For this hybrid instrument, the monolithic telescope must complete the frequency coverage $\{8, \ldots, 22\}$ by measuring the continuous spectrum $[0, 8]$. In contrast to SPIDER's frequency coverage presented in Fig. 2, we would measure all spatial frequencies from 0 to 22 whereas SPIDER has 11 missing spatial frequencies in this range $\{7, 9, 11, 12, 14, 15, 16, 18, 19, 20, 21\}$. To sum up, we would achieve a compact frequency coverage up to the spatial frequency 22 and would improve the PRL with respect to the SPIDER configuration.

We now aim at dimensioning the monolithic telescope and deriving under which condition it fits at the center of the interferometer.

As can be observed in Fig. 1, the central space may be used to install the monolithic telescope. Let us look at the conditions under which the low frequencies that are not measured by the arms may be recorded with this telescope.

The maximum frequency measured by the telescope is fixed by its diameter, itself necessarily smaller than the diameter of this central space, D_{in}.

To calculate this diameter, we must make some additional assumptions about the arms. First, we assume that the diameter of the apertures, d, is equal to the distance between apertures, b. Secondly, we consider the arms positioned in such a way that the apertures of the first ring are joint.

Under these assumptions, the perimeter of the circle going through the center of each aperture is $P = \pi(D_{\mathrm{in}} + d)$. Secondly, the perimeter of the regular polygon whose vertices are the centers of each aperture, if the first apertures of each arm are touching one another, is $P' = N_a d$, with N_a the number of interferometric arms. Thus, we have approximately $P' = P$, yielding

$$D_{\mathrm{in}} = d(N_a/\pi - 1). \tag{3}$$

Hence, the monolithic telescope measures continuous spatial frequencies up to $d/b \times (N_a/\pi - 1)$. As we consider our apertures to be joint, i.e., $d = b$, the spatial frequencies measured by the monolithic telescope span up to $N_a/\pi - 1$.

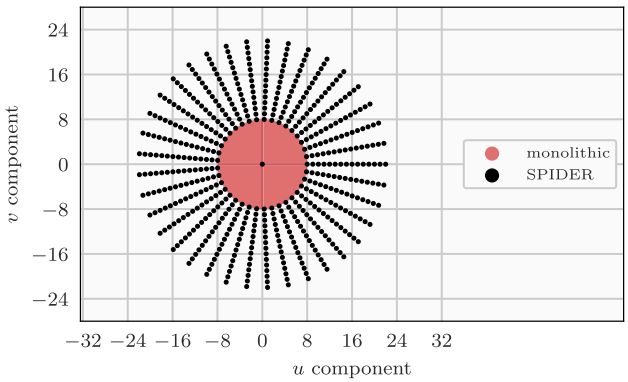

Fig. 5. Optical transfer function of the suggested hybrid instrument with a monolithic telescope complemented by a SPIDER-like instrument with radially disposed arms. The monolithic measures the continuous spatial frequencies $[1, 8]$ (red) and the interferometer spatial frequencies $\{8, \ldots, 22\}$ (black).

To ensure that there is no gap between the spatial frequencies measured by the monolithic telescope and the interferometer, the maximum spatial frequency measured by the monolithic telescope must be equal to or greater than the minimum spatial frequency measurement by the interferometer. In other words, we need

$$D_{\text{in}} \geq n_{\text{min}}^{\text{max}} b. \tag{4}$$

Considering Eq. (3), and injecting the expression of $n_{\text{min}}^{\text{max}}$ from Eq. (2) in Eq. (), we obtain the following inequality:

$$N_{\text{a}} \geq \pi \lfloor (N_{\text{p}} + 6)/4 \rfloor. \tag{5}$$

In the particular case of the SPIDER-like design presented in Fig. 2 with $N_{\text{a}} = 37$ and $N_{\text{p}} = 30$, this condition is verified, allowing the monolithic telescope to be placed at the center of the interferometer and measuring the necessary missing low spatial frequencies. Finally, the two-dimensional optical transfer function resulting from the combination of the monolithic telescope and SPIDER-like interferometer is presented in Fig. 5.

In summary, we have proposed an original method allowing one to determine whether or not a compact frequency coverage is buildable, given the number of apertures and the lowest sought spatial frequency. The solution is constructive and does not require a computationally costly systematic exploration, making our approach fit to interferometric arms with a large number of apertures. This tool allowed us firstly to propose a rewiring of the SPIDER architecture, achieving a compact frequency coverage. We then used it to suggest a hybrid architecture combining a small monolithic aperture, for low spatial frequency measurements, placed at the center of a SPIDER-like instrument that measures higher spatial frequencies and still achieves a compact frequency coverage. The methodology used is transposable to any two-dimensional instrument composed of a set of linear interferometric arms.

Acknowledgments. The authors acknowledge the useful discussions with Sébastien Lopez from Airbus Defence and Space.

Disclosures. The authors declare no conflicts of interest.

Data availability. Simulation code is available in Code 1 Ref. [27].

REFERENCES

1. A. A. Michelson and F. G. Pease, Proc. Natl. Acad. Sci. U. S. A. **7**, 143 (1921).
2. W. J. Tango and R. Twiss, *Progress in Optics* (Elsevier, 1980), Vol. 17, pp. 239–277.
3. J.-M. Mariotti, *Diffraction-Limited Imaging with Very Large Telescopes* (Springer, 1989), pp. 3–32.
4. R. G. Petrov, F. Malbet, and G. Weigelt, *et al.*, A&A **464**, 1 (2007).
5. J. T. Armstrong, D. Mozurkewich, L. J. Rickard, D. J. Hutter, J. A. Benson, P. Bowers, N. Elias II, C. Hummel, K. Johnston, D. Buscher, J. H. Clark, L. Ha, L.-C. Ling, N. M. White, and R. S. Simon, Astrophys. J. **496**, 550 (1998).
6. H. McAlister, T. ten Brummelaar, D. Gies, W. Huang, W. Bagnuolo Jr, M. Shure, J. Sturmann, L. Sturmann, N. Turner, S. Taylor, D. H. Berger, E. K. Baines, E. Grundstrom, C. Ogden, S. T. Ridgway, and G. van Belle, Astrophys. J. **628**, 439 (2005).
7. M. Malbet, J. Schanen-Duport, J. Berger, K. Rousselet-Perraut, P. Benech, and P. Kern, Astron. Astrophys. **348**, 1055 (1999).
8. R. L. Kendrick, A. Duncan, C. Ogden, J. Wilm, D. M. Stubbs, S. T. Thurman, T. Su, R. P. Scott, and S. Yoo, in *Advanced Maui Optical and Space Surveillance Technologies Conference* (AMOS, 2013), E45.
9. A. L. Duncan and R. L. Kendrick, "Segmented planar imaging detector for electro-optic reconnaissance," U.S. patent 8913859 (16 December 2014).
10. T. Su, R. P. Scott, C. Ogden, S. T. Thurman, R. L. Kendrick, A. Duncan, R. Yu, and S. Yoo, Opt. Express **25**, 12653 (2017).
11. T. Su, G. Liu, K. E. Badham, S. T. Thurman, R. L. Kendrick, A. Duncan, D. Wuchenich, C. Ogden, G. Chriqui, S. Feng, J. Chun, W. Lai, and S. J. B. Yoo, Opt. Express **26**, 12801 (2018).
12. K. Badham, R. L. Kendrick, D. Wuchenich, C. Ogden, G. Chriqui, A. Duncan, S. T. Thurman, S. J. B. Yoo, T. Su, W. Lai, J. Chun, S. Li, and G. Liu, in *2017 Conference on Lasers and Electro-Optics Pacific Rim (CLEO-PR)* (IEEE, 2017), pp. 1–5.
13. J. E. Harvey and R. A. Rockwell, Opt. Eng. **27**, 279762 (1988).
14. L. Damé and M. Martic, in *Proceedings of the ESA Colloquium* (European Space Agency, 1992), pp. 201–208.
15. L. M. Mugnier, G. Rousset, and F. Cassaing, J. Opt. Soc. Am. A **13**, 2367 (1996).
16. Q. Chu, Y. Shen, M. Yuan, and M. Gong, Opt. Commun. **405**, 288 (2017).
17. G.-M. Lv, Q. Li, Y.-T. Chen, H.-J. Feng, Z.-H. Xu, and J. Mu, Opt. Rev. **26**, 664 (2019).
18. K. Cao, Z. Ye, C. Jiang, J. Zhu, Z. Qiao, and Y. Jiang, Opt. Eng. **59**, 043105 (2020).
19. C. Ding, X. Zhang, X. Liu, H. Meng, and M. Xu, IEEE Access **8**, 139396 (2020).
20. G. Liu, D. Wen, W. Fan, Z. Song, B. Li, and T. Jiang, Opt. Express **30**, 4905 (2022).
21. G. Nordh, Discret. Math. **308**, 1653 (2008).
22. T. Skolem, Math. Scand. **6**, 273 (1958).
23. R. O. Davies, Math. Gaz. **43**, 253 (1959).
24. J.-C. Bermond, A. E. Brouwer, and A. Germa, in *Problèmes Combinatoires et Théorie des Graphes, Colloque International CNRS 260* (CNRS, 1978), Vol. 260, pp. 35–38.
25. J. E. Simpson, Discret. Math. **44**, 97 (1983).
26. C. D. Langford, Math. Gaz. **42**, 228 (1958).
27. H. Debary, "Python code providing optimal aperture configurations of an interferometric telescope for extended scene observation," figshare (2022), https://doi.org/10.6084/m9.figshare.20440353.